



## Letters to the Editor

### Paediatric enterovirus meningitis without cerebrospinal fluid pleocytosis



Dear editor, we read with interest the article (Multiplex PCR reveals high prevalence of enterovirus and HHV6 in acellular paediatric cerebrospinal fluid samples) by Lumley et al. published in this journal<sup>1</sup>. We would like to share our experience with Enterovirus meningitis without pleocytosis in paediatrics.

EV are the most common cause of viral meningitis (VM) in all ages, and account for 90% of VM in infants<sup>2</sup>. EV meningitis (EVM) is defined by the presence of CSF pleocytosis and detection of EV genome in CSF using molecular techniques<sup>3</sup>. Since the introduction of molecular methods for virus detection in routine, an increase of EVM incidence has been reported due to higher sensitivity<sup>4</sup>.

Previous studies reported EVM without CSF pleocytosis, especially in children, suggesting that CSF pleocytosis should not be a mandatory criterion for the diagnosis of EVM<sup>3</sup>.

This study aimed to investigate the factors associated with EVM cases without CSF pleocytosis.

A retrospective study was conducted at the university hospital of Lille from 1 January 2013 to 31 December 2018. Patients (< 17 years old) from the different paediatric wards with a clinical suspicion of meningitis, and who underwent a CSF analysis including EV detection by RT-PCR, were included in the study.

Pleocytosis was defined as an elevation of leukocyte count in CSF. The age-dependant pleocytosis definition was: leukocytes > 15/mm<sup>3</sup> (< 3 months), > 8 leukocytes/mm<sup>3</sup> (between 3 months – 3 years), and > 5 leukocytes/mm<sup>3</sup> (>3 years old).

Data from a total of 780 paediatric patients were initially collected. EV was detected in CSF for 141 patients (18%). Clinical and laboratory findings were summarized in Table 1. Fifty-five patients (39%) with EVM in our study did not present CSF pleocytosis. The absence of CSF pleocytosis was more common in younger patients (Table 2). The proportion of patients without CSF pleocytosis was 84% in newborns, and decreased to 59% in patients aged from 1 month to 3 years, and reached 19% in patients older than three years. Neurological and gastrointestinal signs and symptoms were less common in patients without CSF pleocytosis. Neither length of stay in the hospital nor the delay between the onset of clinical manifestations and lumbar puncture were significantly different. Fewer antibiotics were prescribed for patients without CSF pleocytosis. Lower blood leukocytes counts and higher CRP level were noted in patients without CSF pleocytosis. In the multivariate analysis, the absence of CSF pleocytosis was independently associated with younger age and higher CRP level (Table 2).

This study highlights that the absence of CSF pleocytosis during EVM is common in children (39%). Since the introduction of molecular techniques for virus detection, few reports have described the lack of CSF pleocytosis in confirmed EVM cases in paediatrics<sup>3,5</sup>.

Despite the variations in CSF pleocytosis definition and the age of paediatric populations in those articles, it is obvious that the rate of detection of EVM cases without pleocytosis has increased in recent years. This increase in the rate of detection can be explained by the fact that EV detection molecular methods have gained a higher sensitivity and rapidity.

The exact mechanism of the absence of CSF pleocytosis in EMV is unknown and remains to be elucidated. However, Seiden et al. suggested that the absence of CSF pleocytosis is probably explained by the immaturity of the immune system and its ability to create an inflammatory reaction to EV infections in young children<sup>6</sup>. Moreover, Mulford et al. postulated that the late chemokine response, which is required for leukocyte activation at the site of infection, has not been well developed in these children<sup>7</sup>. Clinically, neurological and digestive manifestations were less common in patients without CSF pleocytosis. This observed association could be due to an age-related bias in our study, as 40% of our patients were younger than two years. However, this finding is still consistent with a recent article<sup>5</sup> showed that fever, headache and vomiting were less common in patients with CSF non pleocytosis. In our findings, 35% of patients in confirmed EVM cases have received antibiotics (in the absence of documented bacterial infection), 18% of those patients presented without CSF pleocytosis. These results might be linked to a lack of confidence and comfort of the clinicians to avoid antibiotic prescription and discharge patients earlier. Therefore, the benefit of detecting EV by a rapid molecular method is not limited to the early diagnosis. It enables rapid discontinuation of antibiotics, unnecessary additional tests and early discharge from hospital all of which are reassuring for the patients' families.

Lower blood leukocytes and higher CRP level were the major laboratory findings associated with EVM without CSF pleocytosis. This result is coherent with a previous study<sup>3</sup>. The inverse proportional relationship, between blood leukocytes counts and CRP level in the patients without CSF pleocytosis, has been studied<sup>8</sup>. Sato et al. found that the negative correlation between WBCs and CRP might be an early (or initial) stage of infection that starts with the release of pro-inflammatory cytokines, before blood leukocytes production and penetration of the blood-brain barrier.

In conclusion, the proportion of EVM cases without CSF pleocytosis is important. This confirms the importance of EV screening in the suspected cases of meningitis even in the absence of CSF pleocytosis. Hence, rapid detection of EV has a significant clinical impact and molecular methods are currently available in routine in most of clinical laboratories.

#### Funding source

The authors received no specific funding for this work.

**Table 1**  
General characteristics and laboratory findings of patients with EV meningitis.

| Finding  | % Patients with EV meningitis (n) (n = 141) |
|--|---|
| Fever  | 91% (129)                                   |
| Neurological Manifestations  | 60% (84)                                    |
| Gastrointestinal Manifestations  | 59% (83)                                    |
| Respiratory Manifestations   | 20% (29)                                    |
| Dermatological Manifestations  | 14% (20)                                    |
| Children received antibiotics  | 35% (50)                                    |
| Length of stay (hours) (median ± IQR)  | 36±51                                       |
| Delay between clinical manifestations and lumbar puncture (hours) (median ± IQR) | 24±36                                       |
| Blood Leukocytes /mm <sup>3</sup> (median, range)                                | 11 (2–34)                                   |
| CRP mg/L (median, range)   | 7 (3–75)                                    |
| CSF Leukocytes/mm <sup>3</sup> (median, range)                                   | 12 (0–1280)                                 |

IQR: Interquartile range. CRP: C-reactive protein. CSF: cerebrospinal fluid.

**Table 2**  
Univariate and multivariate analyses testing clinical and laboratory factors significantly associated with absence of CSF pleocytosis.

| Finding                                       | Univariate analysis <sup>§</sup>     |                                   |                      | Multivariate analysis <sup>§§</sup> |               |
|---|--------------------------------------|-----------------------------------|----------------------|-------------------------------------|---------------|
|   | EVM without CSF pleocytosis (n = 55) | EVM with CSF pleocytosis (n = 86) | p value <sup>#</sup> | aOR                                 | 95% CI        |
| Age (Month) (mean ± SD)                       | 22±33                                | 66±49                             | <0.0001*             | 0.980**                             | 0.962 – 0.998 |
| Neurological manifestations                   | 31%                                  | 80%                               | <0.0001*             | –                                   | –             |
| Digestive manifestations                      | 44%                                  | 71%                               | <0.001*              | –                                   | –             |
| Antibiotics prescription                      | 25%                                  | 42%                               | 0.0406*              | –                                   | –             |
| Blood leukocytes /mm <sup>3</sup> (mean ± SD) | 10±5                                 | 12±4.7                            | 0.022*               | –                                   | –             |
| CRP mg/L (mean ± SD)                          | 15±16                                | 10±9.4                            | 0.019*               | 1.045**                             | 1.007– 1.083  |
| CSF leukocytes /mm <sup>3</sup> (mean)        | 3                                    | 123                               | <0.0001*             | –                                   | –             |

SD: Standard deviation. aOR: adjusted odds ratio. CI: confidence interval. CRP: C-reactive protein. CSF: cerebrospinal fluid.

<sup>#</sup> The alpha criterion for p-value was set to 0.05.

\* Significant in univariate analysis.

\*\* Significant in multivariate analysis.

§ Chi-square test and t-test were used for univariate analysis.

§§ Multiple logistic regression was used for multivariate analysis using the factors significantly associated with the absence of CSF pleocytosis in univariate analysis.

## Financial disclosure

The authors have no financial relationships relevant to this article to disclose.

## Declaration of Competing Interest

The authors have no conflicts of interest to disclose.

## References

- [1] Lumley S.F., Pritchard D., Dutta A., Matthews P.C., Cann K. Multiplex PCR reveals high prevalence of enterovirus and HHV6 in acellular paediatric cerebrospinal fluid samples. *J Infect* 2018;**77**(3):249–57.
- [2] Huang C., Morse D., Slater B., Anand M., Tobin E., Smith P., et al. Multiple-Year experience in the diagnosis of viral central nervous system infections with a panel of polymerase chain reaction assays for detection of 11 viruses. *Clinical Infectious Diseases* 2004;**39**(5):630–5.
- [3] de Crom S.C., van Furth M.A., Peeters M.F., Rossen J.W., Obihara C.C. Characteristics of pediatric patients with enterovirus meningitis and no cerebral fluid pleocytosis. *Eur J Pediatr* 2012;**171**(5):795–800.
- [4] Harvala H., Simmonds P. Viral meningitis: epidemiology and diagnosis. *Lancet Infect Dis* 2016;**16**(11):1211–12.
- [5] Song J.Y., Nam S.O., Kim Y.A., Kim K.M., Lyu S.Y., Ko A., et al. Cerebrospinal fluid non-pleocytosis in pediatric enteroviral meningitis: large-scale review. *Pediatrics Int*. 2018;**60**(9):855–61.
- [6] Seiden J.A., Zorc J.J., Hodinka R.L., Shah S.S. Lack of cerebrospinal fluid pleocytosis in young infants with enterovirus infections of the central nervous system. *Pediatr Emerg Care* 2010;**26**(2).
- [7] Mulford W.S., Buller R.S., Arens M.Q., Storch G.A. Correlation of cerebrospinal fluid (CSF) cell counts and elevated csf protein levels with enterovirus reverse transcription-PCR results in pediatric and adult patients. *J. Clin. Microbiol.* 2004;**42**(9):4199–203.
- [8] Sato M., Hosoya M., Honzumi K., Watanabe M., Ninomiya N., Shigeta S., et al. Cytokine and cellular inflammatory sequence in enteroviral meningitis. *Pediatrics* 2003;**112**(5):1103.

Abdulaziz Alhazmi  
 Université de Lille Faculté de Médecine CHU Lille Laboratoire de  
 Virologie, EA3610 F-59037, Lille, France  
 Microbiology Department, Jazan University, Jazan, Saudi Arabia  
 Mouna Lazrek, Enagnon Kazali Alidjinou, Guillaume Descombes,  
 Ilka Engelmann, Didier Hober\*  
 Université de Lille Faculté de Médecine CHU Lille Laboratoire de  
 Virologie, EA3610 F-59037, Lille, France

\*Corresponding author.

E-mail address: [didier.hober@chru-lille.fr](mailto:didier.hober@chru-lille.fr) (D. Hober)

Accepted 8 November 2019  
 Available online 13 November 2019

<https://doi.org/10.1016/j.jinf.2019.11.006>

© 2019 The British Infection Association. Published by Elsevier Ltd. All rights reserved.

## Transmitted and acquired oseltamivir resistance during the 2018–2019 influenza season



Dear Editor,

Recent studies highlight the complex mechanisms underlying influenza seasonality,<sup>1</sup> as well as the problems around early,

accurate diagnostic testing of influenza in hospitalised patients at the bedside.<sup>2</sup> The additional component of this influenza puzzle is the role and impact of antiviral therapy.

Each year Public Health England (PHE) updates its seasonal influenza guidance, which usually includes a recommendation to consider the use of zanamivir instead of oseltamivir in the immunocompromised. This is particularly important when influenza A(H1N1)pdm09 is circulating, due to its lower threshold for developing the neuraminidase (NA) H275Y oseltamivir drug resistance mutation.<sup>3</sup> The influenza season in Leicester, UK tends to start late in the year, around November–December, peaking in January–February, and ending in March–April.<sup>4</sup>

During the 2018–2019 influenza season, which was dominated by influenza A(H1N1)pdm09, we were informed by PHE Colindale (the UK influenza reference laboratory) of three cases of H275Y-associated oseltamivir drug resistant influenza A(H1N1)pdm09 viruses present in clinical samples that were obtained in Nov 2018 (Case 1), Jan 2019 (Case 2) and Feb 2019 (Case 3). Each of these cases differed in their duration of oseltamivir treatment and clinical background:

Case 1: was a 39-year old woman with a history of mild asthma, who presented to the emergency department with a 4-day history of coryzal symptoms. She lived with an 18-year old daughter and a 13-month old toddler, who had just started attending nursery. None of these children had been tested nor treated for influenza, though the toddler had been seen by the GP four days earlier and been prescribed some antibiotics for acute otitis media. Sequencing of the influenza A(H1N1)pdm09 virus obtained from a throat swab from case 1 showed 100% H275Y viral population by whole genome sequencing (WGS) using next generation methods (CASE1\_A/ENG/620/2018\_2018-11-14) (Fig. S1). She had not been treated with oseltamivir before the sample was taken, suggesting a possible case of either transmitted H275Y drug resistance or a spontaneous H275Y mutation. She was admitted to the respiratory ward then discharged the next day on clarithromycin 500 mg BD PO and oseltamivir 5 days 75 mg BD PO, as it was unknown at that time that her influenza virus was oseltamivir resistant.

Case 2: was a 15-month old girl with Nager syndrome (a rare condition affecting the development of the face, hands, arms, typically resulting in various degrees of malar hypoplasia and micrognathia, but is not known to be immunocompromising). She had been admitted to paediatric intensive care (PICU), after being transferred from another local hospital, where she had already had 5 days of oseltamivir treatment for laboratory-confirmed influenza A(H1N1)pdm09 infection. She was still positive for influenza in a nasopharyngeal aspirate (NPA – later sent for sequencing: CASE2\_A/ENG/22/2019\_2019-01-05) (Fig. S1) after transfer, 6 days after onset of her influenza infection, and therefore received another 10 days of oseltamivir treatment on our PICU. As there was little clinical improvement in her condition, and the influenza A(H1N1)pdm09 infection was persisting, a recommendation was made to switch to intravenous zanamivir, empirically (i.e. before the viral sequencing results were available from PHE), but unfortunately, this child died soon after on PICU due to respiratory complications related to her influenza infection and concomitant secondary bacterial pneumonia. She had two samples (taken 5–6 days after starting oseltamivir) that were sequenced by PHE, which showed an increasing population of drug-resistant (H275Y positive) viruses from 35% to 80% on two consecutive days using WGS): (CASE2\_A/ENG/22/2019\_2019-01-05; CASE2\_A/ENG/70/2019\_2019-01-06) (Fig. S1).

Case 3: was a 7-week old infant boy admitted with fever (up to 38.6 °C), poor feeding and mottled skin with signs of peripheral shut-down. His-mother was also suffering from a febrile illness which was causing her nausea and vomiting, but she was not

tested or treated for influenza infection. He was admitted to the paediatric ward for observation and to re-establish feeding, and started on a 5-day empirical course of intravenous antibiotics and oseltamivir. After 4 days, influenza A(H1N1)pdm09 infection was confirmed on an NPA, but as he was now clinically well, he was discharged home to finish his antiviral treatment. Follow-up viral sequencing at the PHE laboratory demonstrated a 44% H275Y viral population (CASE3\_A/ENG/288/2019\_2019-02-18) (Fig. S1).

A phylogenetic analysis of these H275Y-containing NA gene sequences and those from other circulating strains published in GSAID (<https://www.gisaid.org/>) showed that these three reported cases are not clustered closely together, suggesting that they are independent cases (Fig. S1). Note that this tree was constructed without the H275Y codon, so there is no impact of this drug resistance mutation on the tree topology.

Based on Fig. S1, Case 1's virus is most closely related to similar viruses from the USA (2018–2019) and Australia (2018), none of which contained the H275Y mutation. Case 2's virus is grouped most closely with European viruses (Spain 2019, Sweden 2019, France 2018), and slightly more distantly, with viruses from England (2019), of which one (A/England/81/2019; from Manchester) also contained the H275Y mutation. However, these viruses may not have been epidemiologically related. Case 3's virus is grouped with a large cluster including mostly 2019 A(H1N1)pdm09 viruses from the USA, Europe, Asia, where many of these viruses branch off the same trunk, so no unique common ancestor is easily determined. Several of these viruses contain the H275Y mutation, including some from the USA and one from England (A/England/2/2019; from London). However, again, these may not necessarily be related epidemiologically.

This case series re-emphasises several important aspects of the PHE guidance in a real-life hospital setting: (i) that the oseltamivir H275Y drug resistance-associated mutation (DRM) in influenza A(H1N1)pdm09 subtype viruses can be present with the potential to be transmitted, relatively early on in the season; (ii) that the oseltamivir H275Y DRM can appear during both the standard 5-day and prolonged 10-day treatment course; (iii) that earlier, more rapid (e.g. on-site) viral sequencing and identification of the H275Y DRM (e.g. by specific PCR detection of this mutation in clinical samples) has the potential to impact on clinical management in real-time, e.g. allowing an earlier switch to zanamivir as an alternative antiviral treatment for influenza.<sup>3</sup>

#### Conflict of interest statement

None.

#### Supplementary material

Supplementary material associated with this article can be found, in the online version, at doi:10.1016/j.jinf.2019.10.020.

#### References

- Lam T.T., Tang J.W., Lai F.Y., Zaraket H., Dbaibo G., Bialasiewicz S., et al. INSPIRE (International network for the sequencing of respiratory viruses). Comparative global epidemiology of influenza, respiratory syncytial and parainfluenza viruses, 2010–2015. *J Infect* 2019;**79**(4):373–82. doi:10.1016/j.jinf.2019.07.008.
- Tang J.W., Blount J., Bradley C., Donaghy B., Shardlow C., Bandi S., et al. Impact of a poorly performing point-of-care test during the 2017–2018 influenza season. *J Infect* 2019;**78**(3):249–59. doi:10.1016/j.jinf.2018.10.013.
- PHE guidance on use of antiviral agents for the treatment and prophylaxis of seasonal influenza. Version 9.1, January 2019. [https://assets.publishing.service.gov.uk/government/uploads/system/uploads/attachment\\_data/file/773369/PHE\\_guidance\\_antivirals\\_influenza.pdf](https://assets.publishing.service.gov.uk/government/uploads/system/uploads/attachment_data/file/773369/PHE_guidance_antivirals_influenza.pdf) (Accessed 18 Aug 2019).
- Tang J.W., Mutuyimana J., Teo K.W., Lea S., Galiano M., Lackenby A., et al. Early seasonal influenza vaccination and delayed influenza peaks – a possible cause of end-of-season outbreaks. *J Infect* 2018;**76**(1):96–8. doi:10.1016/j.jinf.2017.08.002.

Julian W. Tang\*

Clinical Microbiology, University Hospitals of Leicester NHS Trust,  
Level 5 Sandringham Building, Leicester Royal Infirmary, Infirmary  
Square, Leicester LE1 5WW, UK  
Respiratory Sciences, University of Leicester, Leicester, UK

Matthew Kennedy

Clinical Microbiology, University Hospitals of Leicester NHS Trust,  
Level 5 Sandringham Building, Leicester Royal Infirmary, Infirmary  
Square, Leicester LE1 5WW, UK

Angie Lackenby, Joanna Ellis

Respiratory Virus Unit, Public Health England, Colindale, London, UK

Tommy Lam

State Key Laboratory of Emerging Infectious Diseases, School of  
Public Health, The University of Hong Kong, Hong Kong SAR, China

\*Correspondence author at: Clinical Microbiology, University  
Hospitals of Leicester NHS Trust, Level 5 Sandringham Building,  
Leicester Royal Infirmary, Infirmary Square, Leicester LE1 5WW,  
UK.

E-mail address: [julian.tang@uhl-tr.nhs.uk](mailto:julian.tang@uhl-tr.nhs.uk) (J.W. Tang)

Accepted 26 October 2019

Available online 13 November 2019

<https://doi.org/10.1016/j.jinf.2019.10.020>

© 2019 The British Infection Association. Published by Elsevier  
Ltd. All rights reserved.

## Nonindigenous case of Asian Zika virus lineage in Yunnan, China, 2019



Dear Editor,

Recent correspondence in this Journal has highlighted the current threat posed by recently-emerging imported Zika virus (ZIKV) in China.<sup>1</sup> ZIKV is a mosquito-borne virus of the family *Flaviviridae*, genus *flavivirus*, which is primarily transmitted to humans by the bite of infected mosquitoes—*Aedes aegypti* and *Ae. albopictus*.<sup>2</sup> In addition, ZIKV is also transmitted efficiently via non-vector-borne routes, including sexual transmission, transfusion, materno-fetal, and contact with infected body fluids.<sup>3</sup> The common clinical presentations of ZIKV infection are fever, headache, skin rashes, conjunctivitis and arthralgia. Most noteworthy, ZIKV can cause fetal microcephaly, miscarriage and life-threatening Guillain-Barré Syndrome in adults. Thus, ZIKV infection is a major global health concern.<sup>4</sup>

Since the first report of ZIKV outbreak on the Yap Island in 2007, ZIKV has rapidly spread to more than 50 countries and territories in Africa, Americas, Asia and the Pacific.<sup>5</sup> In China, the first case of imported ZIKV infection was found in Yunnan in 2014.<sup>1</sup> Subsequently, several sporadic cases of nonindigenous ZIKV infection have been described.<sup>6</sup> Here, we summarize the virological characteristics of a case of imported ZIKV infection detected in Yunnan, China, 2019.

In June 2019, a 29-year-old male returning from Myanmar to Kunming had fever (37.7 °C), headache, and maculopapular rash, and recovered in a week. ZIKV infection was diagnosed using specific real-time reverse transcription-PCR. The study was approved by the Kunming University of Science and Technology Ethics Committee. The participant supplied written informed con-

sent for specimen collection and subsequent analyses. The complete genome sequences isolated from plasma sample were successfully amplified and sequenced with 13 overlapping fragments, and then the sequence obtained was deposited in GenBank under accession no. MN611472.

The virus was designated YNZIKV02 and its full-length genomes possessed 10,807 nucleotides in length. The 5' and 3' noncoding region (NCR) sequences were 107 and 428 nt long, respectively. The ORF encodes a polyprotein with three structural proteins, capsid (315 nt or 105 aa), premembrane/membrane (561 nt or 187 aa), and envelope (1515 nt or 505 aa), and seven nonstructural proteins, NS1 (1056 nt or 352 aa), NS2A (651 nt or 217 aa), NS2B (417 nt or 139 aa), NS3 (1857 nt or 619 aa), NS4A (381 nt or 127 aa), NS4B (765 nt or 255 aa), and NS5 (2712 nt or 904 aa).

Compared with the nucleotide sequences of the available from the NCBI database, YNZIKV02 virus shared the highest 99.21% nucleotide identity with the Asian lineage strain PF13/251013-18 reported previously in French Polynesia, 2013. Further, Bayesian maximum clade credibility (MCC) tree was reconstructed through BEAST version 1.7.5 under the uncorrelated log-normal relaxed clock model with the GTR+I+G nucleotide substitution model based on the complete polyprotein-coding sequences. Bayesian phylogenetic analysis revealed that two clades were observed for Asian lineage, showing significant posterior probabilities of 1.0, respectively. Clade 1 exhibited a single geographic origin of Malaysia, whereas clade 2 presented a substantial mixture of geographic origins, and clade 2 included sequences from Micronesia, Cambodia, Philippines, China, Thailand, French, Brazil, and so on. YNZIKV02 was classified as clade 2 of Asian lineage.

To further investigate the time of emergence of the Asian lineage, we performed Bayesian molecular clock analyses using the complete polyprotein-coding sequences to estimate the time to the most recent common ancestor (tMRCA). As shown in Fig. 1(A), the estimated tMRCA for the clade 1 and clade 2 were 1964.8 [95% highest probability density (HPD): 1963.1, 1968.0] and 1993.7 95% HPD: (1983.6, 2006.9), respectively. In addition, Fig. 1(B) illustrates the demographic history of clade 2 using Bayesian skyline plot analysis; the effective population size decreased slowly from 2002 to 2012 and then had a fast exponential growth from 2012 to 2015, followed by a stable population size.

To further evaluate pandemic risk, some specific amino acid mutations in the YNZIKV02 viral proteins are shown in Fig. 1(C). Notably, the strain YNZIKV02 possessed 188V in NS1, which contributes to increase the secretion of NS1 into the circulatory system, enhance the uptake of viruses by mosquitoes and also result in increased interferon inhibition by NS1.<sup>7–9</sup> Based on three specific amino acid patterns at the positions 17 in prM protein, 188 in NS1 protein, and 114 in NS5 protein, the strains of the Asian lineage can be mainly classified into four genotypes, including SAM, SVM, NVM and VVM.<sup>7</sup> YNZIKV02 belongs to the SVM strain, which circulated in Southeast Asia and was imported into the Pacific before the French Polynesian outbreak,<sup>9</sup> indicating a typical Southeast Asian epidemic genotype.

In summary, we characterized an imported case of Zika virus (YNZIKV02) in Yunnan, China who was returning to China from Myanmar and the strain YNZIKV02 was classed in SVM genotype of Asian lineage. Of note, this isolate harbored the mutation NS1-188V, which can enhance the host interferon-inducing effect of ZIKV escape, and may increase its popularity and potential human disease. To our knowledge, the strain YNZIKV02 is the second imported case of Asian Zika virus lineage in Yunnan, China. This present study highlights the urgent need for continuous molecular screening and epidemic surveillance for ZIKV and its vectors to prevent future outbreaks of ZIKV infection among the human population of Yunnan.

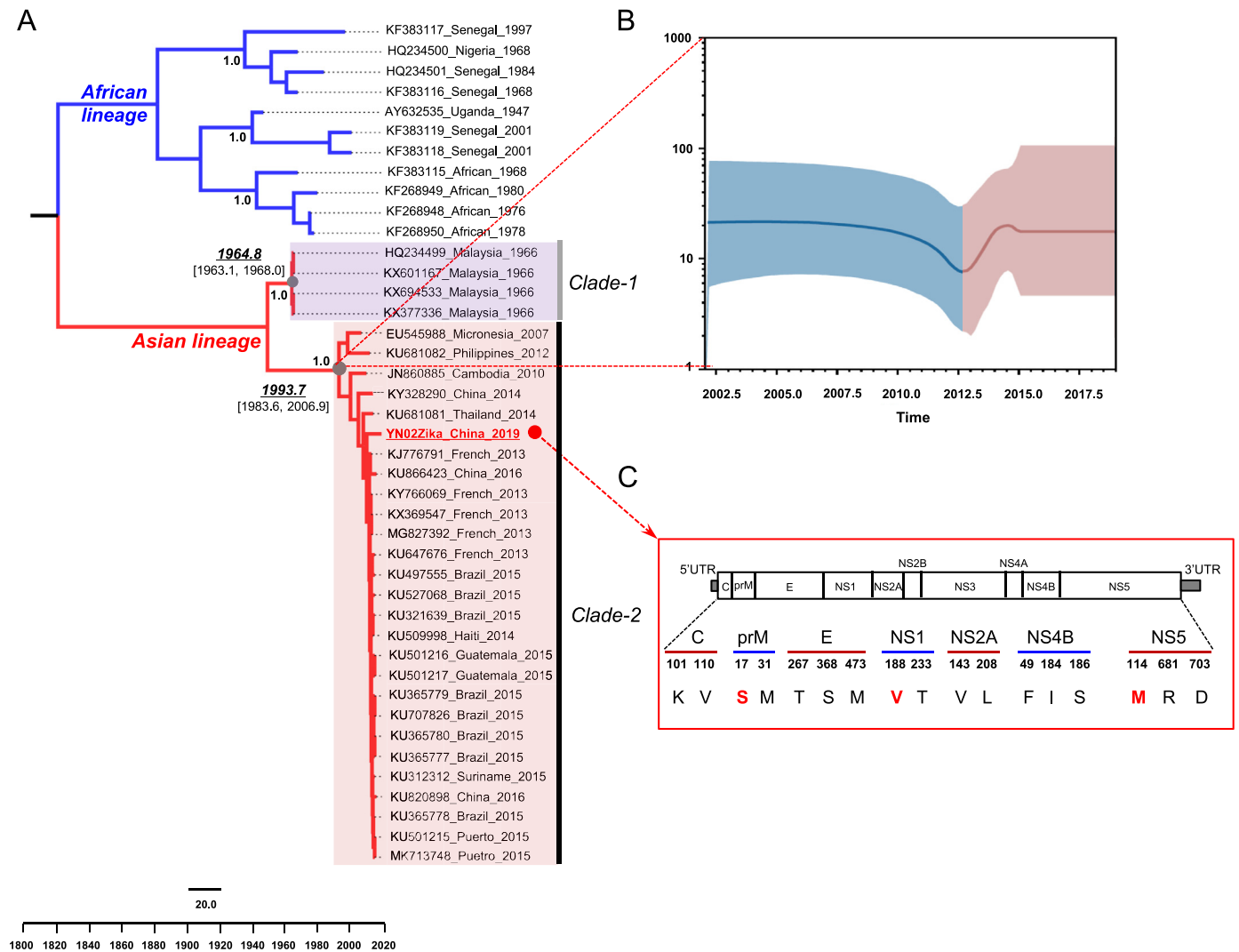


**Fig. 1.** The analyses of Zika virus maximum clade credibility (MCC) trees, Bayesian skyline plot estimated the past population dynamics, and several specific amino acid mutations. (A) Temporal MCC tree of the complete ZIKV coding region sequences obtained from positive plasma sample was constructed based on the uncorrelated log-normal relaxed clock model with the GTR+I+G nucleotide substitution mode. The genotypes of ZIKV were divided into African lineage and Asian lineage. The numbers on the branches represent the posterior probability values. (B) Bayesian skyline plot estimated the past population dynamics of clade-2 of Asian lineage. The y-axis represents the estimates of the effective number of Asian lineage strains and the x-axis represents time. The solid line represents the median estimate and the shaded area represents the 95% confidence intervals. (C) The sequence characteristics of key amino acid residue changes in Zika virus protein. C, capsid; prM, premembrane; NS, nonstructural protein.

## Declaration of Competing Interest

The authors declare no competing financial interests.

## Financial support

This work was supported by the National Natural Science Foundation of China (NSFC) (U1702282), the Reserve Talents Project for Young and Middle-Aged Academic and Technical Leaders of Yunnan Province (2019HB012), and Youth Talent Program of Yunnan “Ten-thousand Talents Program” (YNWR-QNBJ-2018-054).

## Acknowledgments

We thank the members of the Yunnan international travel healthcare center and Kunming Changshui airport customs for the data and sample collection.

## References

- Wang B., Liang Y., Lu Y., Zhang L., Li Y., Song Y., et al. The importation of the phylogenetic-transition state of Zika virus to China in 2014. *J Infect* 2018;**76**(1):106–9.
- Arévalo Romero H., Vargas Pavía T.A., Velázquez Cervantes M.A., Flores Pliego A., Helguera Repetto A.C., León Juárez M. The dual role of the immune response in reproductive organs during Zika virus infection. *Front Immunol* 2019;**10**:1617.
- Baud D., Gubler D.J., Schaub B., Lanteri M.C., Musso D. An update on Zika virus infection. *Lancet* 2017;**390**(10107):2099–109.
- Borges E.D., Vireque A.A., Berteli T.S., Ferreira C.R., Silva A.S., Navarro P.A. An update on the aspects of Zika virus infection on male reproductive system. *J Assist Reprod Genet* 2019;**36**(7):1339–49.
- Deng Y.Q., Zhao H., Li X.F., Zhang N.N., Liu Z.Y., Jiang T., et al. Isolation, identification and genomic characterization of the Asian lineage Zika virus imported to China. *Sci China Life Sci* 2016;**59**(4):428–30.
- Xia H., Wang Y., Atani E., Zhang B., Yuan Z. Mosquito-associated viruses in China. *Virology* 2018;**33**(1):5–20.
- Liu Z.Y., Shi W.F., Qin C.F. The evolution of Zika virus from Asia to the Americas. *Nat Rev Microbiol* 2019;**17**(3):131–9.
- Xia H., Luo H., Shan C., Muruato A.E., Nunes B.T.D., Medeiros D.B.A., et al. An evolutionary NS1 mutation enhances Zika virus evasion of host interferon induction. *Nat Commun* 2018;**9**(1):1–13.

9. Liu Y., Liu J.Y., Du S.Y., Shan C., Nie K.X., Zhang R.D., et al. Evolutionary enhancement of Zika virus infectivity in *Aedes aegypti* mosquitoes. *Nature* 2017;545(7655):482.

Zhili Shen<sup>1</sup>

Faculty of Life Science and Technology, Kunming University of Science and Technology, Kunming, China

Xiaofei Li<sup>1</sup>

Department of Clinical Laboratory, The Third People's Hospital of Kunming City, Kunming, China

Yunlan Lu, Jie Li

Yunnan International Travel Healthcare Center, Kunming, China

Hui Xiao

Faculty of Life Science and Technology, Kunming University of Science and Technology, Kunming, China

Wei Yuan, Ziyang Zhang, Yan Zhou

Kunming Changshui Airport Customs, Kunming, China

Yue Feng\*

Faculty of Life Science and Technology, Kunming University of Science and Technology, Kunming, China

Weihong Qin\*

Yunnan International Travel Healthcare Center, Kunming, China

Xueshan Xia\*

Faculty of Life Science and Technology, Kunming University of Science and Technology, Kunming, China

\*Corresponding authors.

E-mail addresses: [fyky2005@163.com](mailto:fyky2005@163.com) (Y. Feng), [qinwh19@sina.com](mailto:qinwh19@sina.com) (W. Qin), [oliverxia2000@aliyun.com](mailto:oliverxia2000@aliyun.com) (X. Xia)

<sup>1</sup> These first authors contributed equally in this work.

Accepted 28 October 2019

Available online 13 November 2019

<https://doi.org/10.1016/j.jinf.2019.10.023>

© 2019 The British Infection Association. Published by Elsevier Ltd. All rights reserved.

## Emergence and spread of *pvl*-positive genotypic CA-MRSA ST59 with increased adhesion capacity from wounds in hospitals



Dear Editor,

With great interest we read the article by Butler-Laporte et al.,<sup>1</sup> and here we reported the emergence and spread of *pvl*-positive genotypic CA-MRSA ST59 with increased adhesion capacity from wounds in hospitals. Methicillin-resistant *Staphylococcus aureus* (MRSA) has been a major pathogen causing skin and soft tissue infections (SSTIs) and invasive infections in both healthcare and community settings.<sup>1,2</sup> Epidemiological classification and genotypic definition contribute to the understanding of healthcare-associated MRSA (HA-MRSA) and community-associated MRSA (CA-MRSA).<sup>3</sup>

With the dynamic exchange CA-MRSA strains have invaded and spread in hospital settings.<sup>4,5</sup> Molecular epidemiology revealed that different genotypes of CA-MRSA had been isolated from hospitals in various parts in the world.<sup>2</sup> For instance, CA-MRSA ST59 was a representative one in China, and this clone usually con-

tained many virulence factors, especially the Pantone-Valentine leukocidin (PVL).<sup>6</sup> Therefore, it is of great significance to acquire a better understanding of the factors or mechanism underlying CA-MRSA circulating in hospitals.<sup>7</sup> In present study, Pantone-Valentine leukocidin-positive CA-MRSA ST59 with increased capacity of adhesion was found circulating among inpatients with wound infections.

In present study, clinical isolates were collected and molecular characterization including multi-locus sequence typing (MLST), SCCmec typing and *spa* typing were performed as previously reported.<sup>4</sup> Genotypic CA-MRSA strains were defined as those carrying SCCmec IV/ V,<sup>4,5</sup> and the presence of *pvl* gene was detected by PCR. Cell adhesion assay was performed using HaCaT cell line. Briefly, approximately  $1 \times 10^4$  cells (100  $\mu$ l) of the HaCaT cell suspension were seeded onto a coverslip placed in a 24-well plate; after incubating bacteria with HaCaT cell at 37 °C with 5% CO<sub>2</sub> for 1 h, each well was washed with PBS and then fixed within 95% ethanol for one hour and the coverslip was taken out for Gram staining. Statistical analysis was conducted by SAS 8.2 (SAS Institute Inc., Cary, NC, USA).

In a retrospective study of 85 clinical *S. aureus* isolates from burn wounds, one *pvl*-positive isolate of CA-MRSA characterized ST338-SCCmecV-t437 was found as previously reported.<sup>8</sup> This warrants the emergence of CA-MRSA strains in hospitalized patients with wound infections. Then we further performed a prospective study in eight hospitals (discovery cohort), which included a total of 208 MRSA strains from inpatients with wound infection, and data of molecular epidemiology revealed the spread of *pvl*-positive CA-MRSA clone sharing the genotype ST59-SCCmecIV-t441 among inpatients in multiple hospitals in spite of the fact that ST239-SCCmecIII-t030/t037 was the predominant clone circulating in healthcare-associated settings in China (Fig. 1A). This provides the molecular evidence of invasion and transmission of *pvl*-positive CA-MRSA strains into hospital settings and proves the co-existence of CA-MRSA and HA-MRSA in healthcare-associated settings. Next, by targeting *pvl*-positive CA-MRSA strains we analyzed a new cohort of MRSA strains from another tertiary hospital (validation cohort), molecular characterization verified the emergence and invasion of CA-MRSA strains and the transmission of *pvl*-positive CA-MRSA clone, especially the epidemic ST59 CA-MRSA clone (Fig. 1B).

Then we sought to find the reason why ST59 CA-MRSA clone could become prevalent among wound infections. By comparing the strain ST59-SCCmecIV-t441 with other CA-MRSA strains on growth parameter and antimicrobial resistance, no significant difference was found to facilitate the reproduction and survival of this epidemic clone (data not shown). Adhesion is the key to infection and transmission,<sup>9</sup> and cell adhesion assay was performed by co-culturing *S. aureus* isolates and HaCaT cell line. Microscopic examination revealed that *pvl*-positive CA-MRSA ST59 showed increased adhesion to epithelial cells (Fig. 2A–H). As shown in Fig. 2, increased numbers of bacteria were observed in *pvl*-positive CA-MRSA group. Moreover, the total number of bacteria adhered on epithelial cells by ten visual fields with 1000  $\times$  oil immersion objective was counted, and average bacteria number of per cell was calculated (Fig. 2I–K). The data proved the increased capacity of adhesion in epidemic *pvl*-positive CA-MRSA compared to *pvl*-negative CA-MRSA and HA-MRSA strains.

It has been reported that ST59-SCCmec IV/V was the major CA-MRSA clone in China. As predicted by a model from Kouyos et al.,<sup>10</sup> CA-MRSA strains would co-exist with HA-MRSA in hospitals. In present study, we found that CA-MRSA strains has invaded into healthcare-associated settings, and molecular characterization revealed that these strains shared the genotype ST59-SCCmecIV/V, which was the prevalent clone. Moreover, we observed the

### A Discovery cohort: Prospective study of 208 MRSA isolates

| Molecular identity     | No. of MRSA | No. of distributing hospitals | Category | <i>pvl</i> gene |
|------------------------|-------------|-------------------------------|----------|-----------------|
| ST239-SCCmec III-t030  | 95          | 8                             | HA-MRSA  | Negative        |
| ST239-SCCmec III-t037  | 45          | 5                             | HA-MRSA  | Negative        |
| ST239-SCCmec III-t632  | 37          | 1                             | HA-MRSA  | Negative        |
| ST59-SCCmec IV-t441    | 15          | 3                             | CA-MRSA  | Positive        |
| ST239-SCCmec III-t5931 | 5           | 1                             | HA-MRSA  | Negative        |
| ST239-SCCmec NT-t4549  | 3           | 1                             | HA-MRSA  | Negative        |
| ST239-SCCmec III-t233  | 1           | 1                             | HA-MRSA  | Negative        |
| ST239-SCCmec III-t1459 | 1           | 1                             | HA-MRSA  | Negative        |
| ST239-SCCmec III-t421  | 1           | 1                             | HA-MRSA  | Negative        |
| ST1294-SCCmec III-t030 | 1           | 1                             | HA-MRSA  | Negative        |
| ST39-SCCmec II-t007    | 1           | 1                             | HA-MRSA  | Negative        |
| ST5-SCCmec IV-t062     | 1           | 1                             | CA-MRSA  | Negative        |
| ST59-SCCmec IV-t437    | 1           | 1                             | CA-MRSA  | Negative        |
| ST630-SCCmec V-t3388   | 1           | 1                             | CA-MRSA  | Negative        |

### B Validation cohort: Prospective target of *pvl*-positive isolate



Fig. 1. *pvl*-positive CA-MRSA epidemic among inpatients with wound infections.

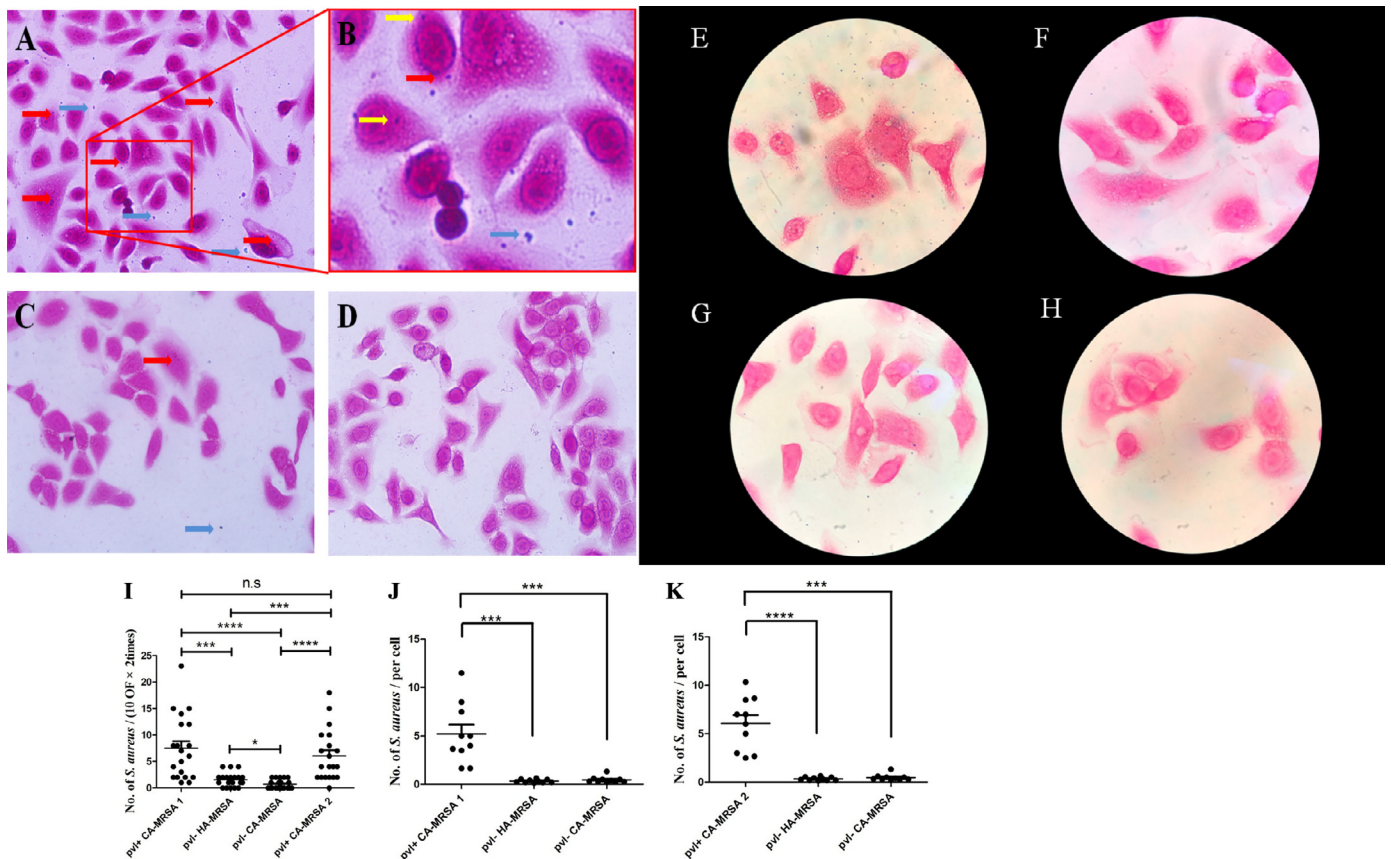


Fig. 2. Increased capacity of adhesion in epidemic *pvl*-positive CA-MRSA. A. Cell adhesion of *pvl*-positive CA-MRSA to HaCaT cell line (400 ×). B. Enlarged part of fig. A, more bacteria seen clearly. C. Cell adhesion of *pvl*-negative CA-MRSA to HaCaT cell line (400 ×). D. Cell adhesion assay negative control, HaCaT cell line only (400 ×). E. Cell adhesion of *pvl*-positive CA-MRSA to HaCaT cell line (oil field). F. Cell adhesion of *pvl*-negative CA-MRSA to HaCaT cell line (oil field). G. Cell adhesion of *pvl*-negative HA-MRSA to HaCaT cell line (oil field). H. Cell adhesion assay negative control, HaCaT cell line only (oil field). I. No. of *S. aureus* adherent to HaCaT cell line were counted on 10 oil fields on two independent occasions; more *pvl*-positive CA-MRSA adherent to HaCaT cell line was found. J. and K. Average No. of *S. aureus* adhered per HaCaT cell was calculated and compared. \* indicated  $p < 0.05$ , \*\*  $p < 0.01$ , \*\*\*  $p < 0.001$ , \*\*\*\*  $p < 0.0001$ , n.s. no significance.

*pvl*-positive ST59 clone circulated in the population with wound infections in 3 out of 8 hospitals in discovery cohort, and verified in another hospital which was a famous center for burns and trauma orthopedic and reconstruction in validation cohort.

Molecular epidemiology implied the *pvl*-positive CA-MRSA ST59 clone may have the potential of circulating in hospitals, but the factors supporting the spread of the strain remain unknown. Then we focused on the adhesion of CA-MRSA strains to epithelial cells. By cell adhesion assay, we found that *pvl*-positive ST59 clone has an advantage in adhesion over other types of MRSA including HA-MRSA and *pvl*-negative CA-MRSA, which may account for the transmission of *pvl*-positive ST59 clone on wound infections. These data contribute to understanding the microbiologic basis of CA-MRSA epidemic among wound infections.

### Ethical approval

This study was approved by Ethics Committee of Shanghai Ninth People's Hospital affiliated to Shanghai Jiao Tong University School of Medicine.

### Declaration of Competing Interest

The authors declare that they have no conflict of interest.

### Acknowledgements

This study was supported by fundamental research program funding of Ninth People's Hospital affiliated to Shanghai Jiao Tong University School of Medicine (No. JYZZ013), Youth program from Shanghai Municipal Commission of Health and Family Planning (No. 20184Y0025), Shanghai Sailing Program (19YF1427500) and the National Natural Science Foundation of China (81870762, 81802303). The authors would thank Peilang Yang (Ruijin hospital, Shanghai Jiao Tong University School of Medicine) for his kind support of HaCaT cell line, Yuxing Ni, Lizhong Han, Changwei Li (Ruijin hospital, Shanghai Jiao Tong University School of Medicine) and Pak-Leung Ho, Wai-U Lo (Queen Mary hospital, The University of Hong Kong) for their help in the experiments.

### Reference

- Butler-Laporte G., De L'Etoile-Morel S., Cheng M.P., McDonald E.G., Lee T.C. MRSA colonization status as a predictor of clinical infection: a systematic review and meta-analysis. *J Infect* 2018;**77**(6):489–95.
- Lakhundi S., Zhang K. Methicillin-resistant *Staphylococcus aureus*: molecular characterization, evolution, and epidemiology. *Clin Microbiol Rev* 2018;**31**(4):e00020–e00018 pii.
- Otter J.A., French G.L. Community-associated methicillin-resistant *Staphylococcus aureus*: the case for a genotypic definition. *J Hosp Infect* 2012;**81**(3):143–8.
- Chen X., Wang W.K., Han L.Z., Liu Y., Zhang H., Tang J., et al. Epidemiological and genetic diversity of *Staphylococcus aureus* causing bloodstream infection in Shanghai, 2009–2011. *PLoS One* 2013;**8**(9):e72811.
- Kateete D.P., Bwanga F., Seni J., Mayanja R., Kigozi E., Mujuni B., et al. CA-MRSA and HA-MRSA coexist in community and hospital settings in Uganda. *Antimicrob Resist Infect Control* 2019;**8**:94.
- Hu Q., Cheng H., Yuan W., Zeng F., Shang W., Tang D., et al. Pantone-Valentine leukocidin (PVL)-positive health care-associated methicillin-resistant *Staphylococcus aureus* isolates are associated with skin and soft tissue infections and colonized mainly by infective PVL-encoding bacteriophages. *J Clin Microbiol* 2015;**53**(1):67–72.
- Feng Y., Chen H.L., Chen C.J., Chen C.L., Chiu C.H. Genome comparisons of two Taiwanese community-associated methicillin-resistant *Staphylococcus aureus* ST59 clones support the multi-origin theory of CA-MRSA. *Infect Genet Evol J Mol Epidemiol Evol Genet Infect Dis* 2017;**54**:60–5.
- Chen X., Yang H.H., Huangfu Y.C., Wang W.K., Liu Y., Ni Y.X., et al. Molecular epidemiologic analysis of *Staphylococcus aureus* isolated from four burn centers. *Burns J Int Soc Burn Inj* 2012;**38**(5):738–42.
- Herman-Bausier P., Labate C., Towell A.M., Derclaye S., Geoghegan J.A., Dufrene Y.F. *Staphylococcus aureus* clumping factor A is a force-sensitive molecular switch that activates bacterial adhesion. *Proc Natl Acad Sci USA* 2018;**115**(21):5564–9.

- Kouyos R., Klein E., Grenfell B. Hospital-community interactions foster coexistence between methicillin-resistant strains of *Staphylococcus aureus*. *PLoS Pathog* 2013;**9**(2):e1003134.

Xu Chen, Kangde Sun, Qingqiong Luo  
Department of Laboratory Medicine, Shanghai Ninth People's Hospital, Shanghai Jiao Tong University School of Medicine (SJTUSM), Shanghai 200011, China

Yantao Duan\*  
Department of Surgery, Shanghai Ninth People's Hospital, Shanghai Jiao Tong University School of Medicine (SJTUSM), Shanghai 200011, China

Fuxiang Chen\*  
Department of Laboratory Medicine, Shanghai Ninth People's Hospital, Shanghai Jiao Tong University School of Medicine (SJTUSM), Shanghai 200011, China  
Faculty of Medical Laboratory Science, Shanghai Jiao Tong University School of Medicine (SJTUSM), Shanghai, 200025, China

\*Corresponding authors.  
E-mail addresses: [sdfcdythewa@163.com](mailto:sdfcdythewa@163.com) (Y. Duan),  
[fuxiang\\_chen@hotmail.com](mailto:fuxiang_chen@hotmail.com) (F. Chen)

Accepted 7 October 2019  
Available online 13 November 2019

<https://doi.org/10.1016/j.jinf.2019.10.005>

© 2019 The British Infection Association. Published by Elsevier Ltd. All rights reserved.

### Characterization of a novel HIV-1 second-generation circulating recombinant form (CRF102\_0107) among men who have sex with men in Anhui, China



Dear Editor,

The high level of genetic variation along with highly recombinogenic reverse transcriptase enzyme of HIV-1 contribute to the emergence of increasing number of circulating recombinant forms (CRFs). Up to date, 101 CRFs have been assigned and published with public sequence data, which is available on the Los Alamos HIV Sequence Database ([www.hiv.lanl.gov](http://www.hiv.lanl.gov)). Most CRFs were found in heterosexual or drug users in the past. Recent correspondence in this Journal has reported on a novel HIV-1 circulation recombinant form (CRF100\_01C) comprising CRF01\_AE and C among heterosexual in Yunnan, China.<sup>1</sup> CRF01\_AE participated in the recombination soon after it became one of the major HIV epidemic strains in China.<sup>2</sup> CRF07\_BC was introduced into men who have sex with men (MSM) population in China at the beginning of the 21st century.<sup>3</sup> Less than 20 years after CRF07\_BC entered China, the second generation CRF (CRF102\_0107) was found in MSM in China. During that time several CRFs and URFs comprising CRF01\_AE and CRF07\_BC lineages were coming out among MSM in Beijing, Jilin, Sichuan, Guangxi, Zhejiang, and Inner Mongolia, China.<sup>3–7</sup> The high frequency of second generation recombination may be due to the higher risk behaviors in MSM, such as unprotected anal intercourse, multiple sexual partners, low rates of condom use and some other factors.

In this study, we defined a novel second-generation CRF (CRF102\_0107) containing 10 segments from subtypes B, C and CRF01\_AE. To analyze its evolutionary history, three epidemiolog-

**Table 1**  
Demographic characteristics of study subjects infected with CRF102\_0107.

| Strain name | Sampling year | Sampling region | Gender | Age | Ethnic group | Marriage | Risk factor | Accession no. |
|-------------|---------------|-----------------|--------|-----|--------------|----------|-------------|---------------|
| FY058       | 2017          | Fuyang, Anhui   | Male   | 40  | Han          | divorced | MSM         | MN178644      |
| FY336       | 2018          | Fuyang, Anhui   | Male   | 28  | Han          | married  | MSM         | MN178645      |
| FY405       | 2018          | Fuyang, Anhui   | Male   | 36  | Han          | divorced | MSM         | MN178646      |

CRF, circulating recombinant form; MSM, men who have sex with men.

ically unlinked HIV-1 positive plasma samples named FY058, FY336 and FY405 were collected from the MSM population in Fuyang, Anhui province. All three participants signed informed consent forms before investigation and peripheral blood collection. The clinical and demographic information are summarized in Table 1.

The near full-length genome (NFLG) of HIV strains were amplified and sequenced. Finally, the NFLG of FY058 and the NFLG of FY336 were successfully amplified. The NFLG of FY058 and FY336 were 8957 bp (HXB2, 623–9,564) and 8,999 bp (HXB2, 608–9,589)

in size, respectively. This two NFLG sequences were submitted to the Basic Local Alignment Search Tool (Blast) for searching for more similar sequences, but no high similarity sequences (>95%) were found. Due to the unsuccessful NFLG amplification of FY405, only a partial sequence of its *pol* region (HXB2, 2253–3,314) was obtained. Considering that more partial genome sequences were submitted to the Los Alamos database than NFLG sequences, the *pol* region sequences of FY405 was used for more blast analysis, and the result showed that no sequences with high similarity

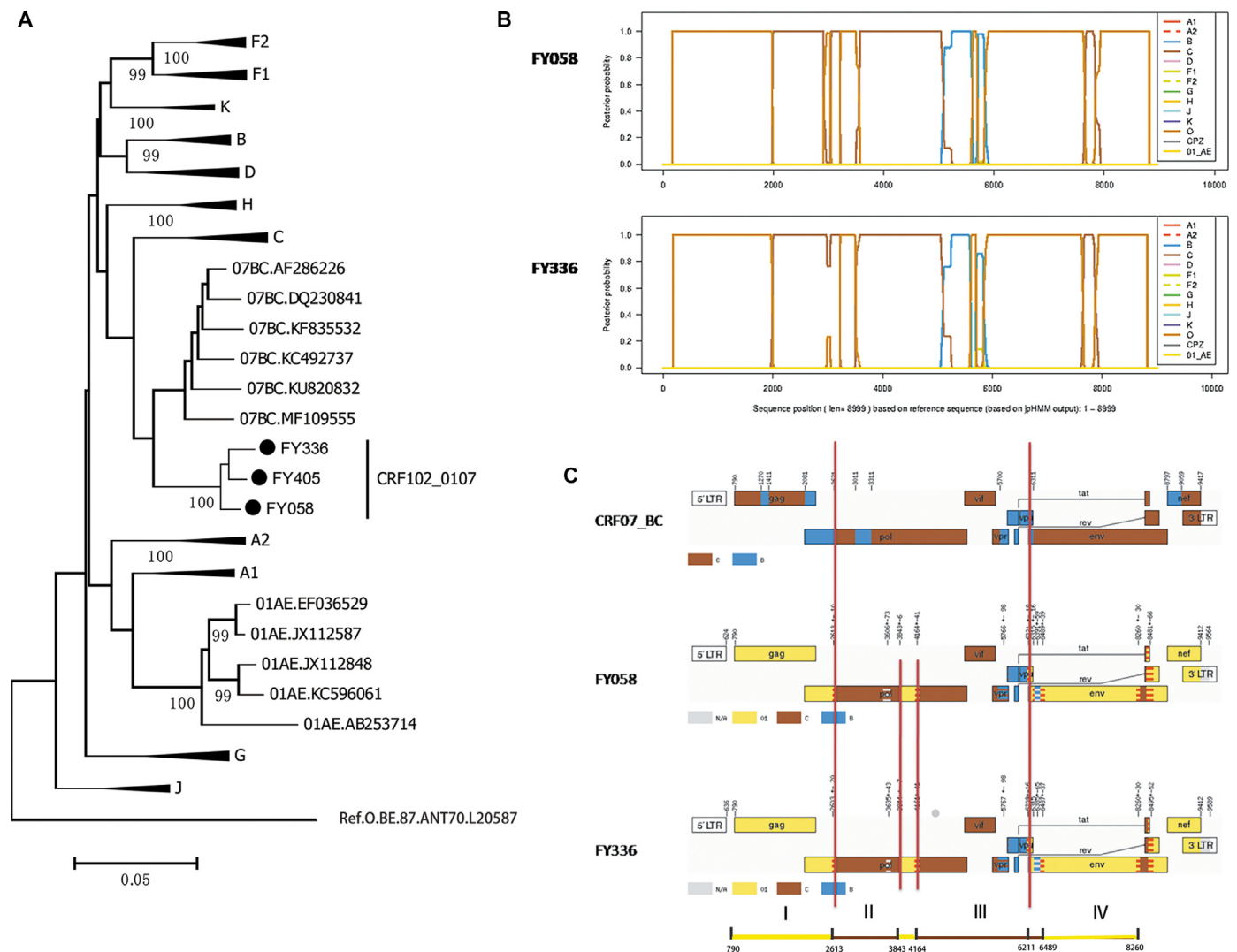


**Fig. 1.** Phylogenetic and recombinant analyses based on near full-length HIV-1 genome sequences. (A) Two NFLG sequences (FY058 and FY336) together with the partial *pol* sequences (2253–3314 nt) of FY405 collected from this study were further aligned with 34 reference sequences which were provided by Foley, Brian Thomas (HIV Databases [bt@lanl.gov](mailto:bt@lanl.gov)), two or more reference strains of each HIV-1 subtype (A1, A2, B, C, D, F1, F2, G, H, J, and K), CRF01\_AE, CRF07\_BC and outgroup O were included. A phylogenetic tree was constructed by the neighbor-joining method based on Kimura 2-parameter model with 1000 bootstrap replicates in MEGA6 software and embellished in Figtree v1.4.4 software. The sequences of CRF102\_0107 were marked with “•”. (B) Recombination breakpoint analysis of CRF102\_0107. (C) Comparison of genomic maps between CRF07\_BC and CRF102\_0107. All these maps were generated using jumping profile hidden Markov model (jpHMM).  
CRF, circulating recombinant form; NFLG, near full-length genome.

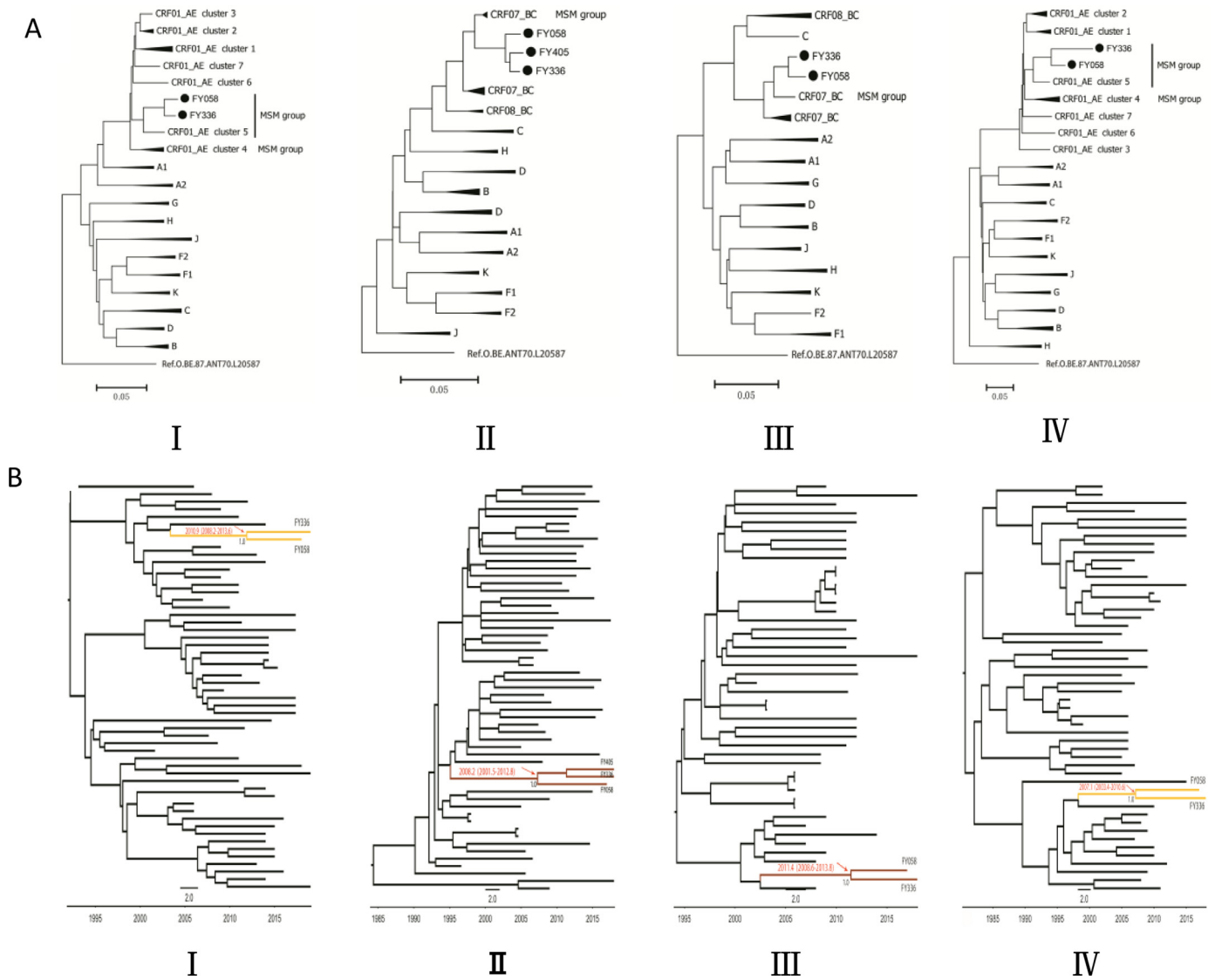


**Fig. 2.** The analyses of CRF102\_0107 subregion trees and maximum clade credibility (MCC) trees. (A) The segment I (HXB2: 790–2613 nt) of the CRF102\_0107 genome map is one of the representative of CRF01\_AE segments inserted into the mosaic structure. The segment II (HXB2: 2613–3843 nt) of the CRF102\_0107 genome map is the representative of CRF07\_BC segments inserted into the mosaic structure. The segment III (HXB2: 4164–6211 nt) of the CRF102\_0107 genome map is another representative of CRF07\_BC segments inserted into the mosaic structure. The segment IV (HXB2: 6489–8260 nt) of the CRF102\_0107 genome map is another representative of CRF01\_AE segments inserted into the mosaic structure. The sequences of CRF102\_0107 were marked with “•”. The methods were described in Fig. 1 and based on the recombinant breakpoints which according to the jpHMM result. (B) MCC trees for the segments (I II III IV) are shown. Timescale is shown at the bottom of the tree. The mean tMRCA and 95% highest probability density (HPD) for the key nodes are indicated. CRF102\_0107 strains are highlighted in yellow (CRF01\_AE) or brown (CRF07\_BC).

(>95%) were found. Two NFLG sequences (FY058 and FY336) together with the *pol* sequences of FY405 were further aligned with 34 reference sequences which were provided by Foley, Brian Thomas (HIV Databases, btf@lanl.gov) including two or more HIV-1 reference strains of each subtype (A1, A2, B, C, D, F1, F2, G, H, J, and K), CRF01\_AE, CRF07\_BC and outgroup O. This alignment was then manually edited using BioEdit v7.2.5 software. A phylogenetic tree was constructed by the neighbor-joining method based on Kimura 2-parameter model with 1000 bootstrap replicates in MEGA6 software and embellished in FigTree v1.4.4 software. For the purpose of recombination analysis, the jumping profile hidden Markov model (jpHMM) ([http://jphmm.gobics.de/submission\\_hiv](http://jphmm.gobics.de/submission_hiv)) was applied. Subsequently, a subregion neighbor-joining tree was constructed to determine the origin cluster of 4 main segments (I II III IV) from CRF01\_AE and CRF07\_BC according to the jpHMM result. Finally, to better understand the time of the most recent common ancestor (tMRCA) of CRF102\_0107, the bayesian molecular clock analyses was performed in BEAST v1.7.5.

The phylogenetic tree showed that the three sequences from epidemiologically unlinked patients formed a distinct monophyletic cluster distinctly related to all known HIV-1 subtypes/CRFs with a high bootstrap value of 100% (Fig. 1A). As shown in the recombination analysis result (Fig. 1B), the two NFLG sequences were composed of CRF01\_AE and subtypes B and C. And the *pol* partial sequence of FY405 shared same breakpoints with FY058 and FY336. Subtype B and C segments of CRF102\_0107 were further submitted for BLAST, the results showed highest similarity to (>95%) CRF07\_BC strains. The comparison of genomic maps between CRF07\_BC and CRF102\_0107 also showed that the BC segments of CRF102\_0107 were highly coincidences with CRF07\_BC (Fig. 1C).

Subregion phylogenetic analyses of 4 genomic segments I (790–2,613 nt), II (2,613–3,843 nt), III (4,164–6,211 nt), IV (6,489–8,260 nt) were further conducted to explore their likely parental lineages. The high bootstrap values in phylogenetic tree supported close relationship with CRF01\_AE or CRF07\_BC subtype references

respectively. Subregion phylogenetic analyses indicated that the segment I and segment IV of CRF102\_0107 belonged to the CRF01\_AE cluster 5, which is mainly circulating among the MSM population in China (Fig. 2A).<sup>8</sup> The segment II and segment III of CRF102\_0107 were clustered with the CRF07\_BC cluster, which was also identified among MSM (Fig. 2A).<sup>3</sup> The segments (I II III IV) of CRF102\_0107 are closely related to the clusters associated with MSM according to the subregional analysis, suggesting that CRF102\_0107 may be predominantly prevalent in the MSM.

The Bayesian analysis shows that the (tMRCA) of the segment I and the segment III from CRF102\_0107 were predicted in 2010.9 [95% highest probability density (HPD): 2008.2, 2013.6] and 2011.4 [95% HPD: (2008.6,2013.8)], respectively (Fig. 2B). The (tMRCA) of the segment II and the segment IV from CRF102\_0107 were predicted in 2008.2 [95% HPD: (2001.5,2012.8)] and 2007.1 [95% highest probability density (HPD): 2003.4, 2010.6], respectively (Fig. 2B). The segments I and III originated around 2010.9–2011.4. The segments II and IV originated around 2007.1–2008.2. Hence, it is speculated that the CRF102\_0107 had been occurred a recombination in two time periods, respectively.

HIV-1 had been increasing rapidly among MSM in China, with the transmission rate of male homosexuality rising from 2.5% in 2006 to 28.0% in 2016 among new cases diagnosed annually. In addition to the rapid spread among MSM, HIV had recently increased in diversity. Several co-circulating subtypes were found in the MSM population, including CRF01\_AE and CRF07\_BC.<sup>3,4,9,10</sup> The prevalence of two or more subtypes in the same population always indicates the emergence of new recombinant strains. The high probability of high-risk sexual behaviors in MSM infected population and other factors, such as unstable sexual partners, higher prevalence rate and genetic diversity in MSM population, which were more possible to occur the recombination and second-generation recombination of HIV-1.<sup>3</sup> In the past studies, multiple CRFs had been reported in MSM population in China. With the rapid spread of CRF07\_BC in MSM in China, CRF01\_AE and CRF07\_BC have become two dominant subtypes among MSM. It is predictable that more and more new second-generation CRFs composed of CRF01\_AE and CRF07\_BC will be defined in the future.

In summary, a novel HIV-1 circulating recombinant form CRF102\_0107 whose genome consists of CRF01\_AE and CRF07\_BC with 9 breakpoints and 10 segments was defined, which has more complex recombinant form than others. The emergence of CRF102\_0107 indicates that CRF01\_AE and CRF07\_BC have been transmitted to individuals with similar social behaviors. The complex social behaviors of MSM infected population will further complicate the molecular epidemic of HIV-1 in China. In recent years, some CRFs and URFs between CRF01\_AE and CRF07\_BC had appeared successively in MSM in China. We can predict that there will be more second-generation CRFs containing CRF01\_AE and CRF07\_BC in the future.

## Funding

This study was supported by the NSFC (81773493), the State Key Laboratory of Pathogen and Biosecurity (AMMS), Anhui provincial Program of Prevent medicine & Public Health (Grant#2017jk002), National Grand Program on Key Infectious Disease Control (Grant#2017ZX10201101).

## Declaration of Competing Interest

The authors declare no competing financial interests.

## Acknowledgments

The authors thank all of the participants, peer workers, and the Fuyang Center for Disease Control and Prevention for the demographic information collection, sample preparation, and testing.

## References

- Feng Y., Zhang C., Zhang M., et al. First report of a novel HIV-1 recombinant form (CRF100\_01C) comprising CRF01\_AE and C among heterosexuals in Yunnan, China. *J Infect* 2018;**77**(6):561–71.
- Guo H., Hu H., Zhou Y., et al. A novel HIV-1 crf01\_ae/b recombinant among men who have sex with men in Jiangsu Province, China. *AIDS Res Hum Retrovir* 2014;**30**(7):706–10.
- Zhang Y., Pei Z., Li H., et al. Characterization of a novel HIV-1 circulating recombinant form (CRF80\_0107) among men who have sex with men in China. *AIDS Res Hum Retrovir* 2019;**35**(4):419–23.
- Li Y., Feng Y., Li F., et al. Genome sequence of a novel HIV-1 circulating recombinant form (CRF79\_0107) identified from Shanxi, China. *AIDS Res Hum Retrovir* 2017;**33**(10):1056–60.
- Wang C., Wang Y., Kong D., et al. Characterization of a novel HIV-1 S-Generation recombinant form in men who have sex with men in Beijing, China. *AIDS Res Hum Retrovir* 2017;**33**(11):1175–9.
- Wang Y., Wei H., Xu W., et al. Identification of a novel CRF01\_ae/CRF07\_bc recombinant form in men who have sex with men in Sichuan, China. *AIDS Res Hum Retrovir* Jul 2016;**32**(7):718–21.
- Jiao Y., Wang Y., Kong D., et al. Characterization of a new HIV-1 CRF01\_AE/CRF07\_BC recombinant virus form among men who have sex with men in Beijing, China. *AIDS Res Hum Retrovir* 2018;**34**(6):550–4.
- Wang X., He X., Zhong P., et al. Phylogenetics of major CRF01\_AE epidemic clusters circulating in mainland of China. *Sci Rep* 2017;**7**(1):6330.
- Zhang X., Li S., Li X., et al. Characterization of HIV-1 subtypes and viral antiretroviral drug resistance in men who have sex with men in Beijing, China. *AIDS* 2007;**21**(Suppl 8):S59–65.
- Han X., An M., Zhang M., et al. Identification of 3 distinct HIV-1 founding strains responsible for expanding epidemic among men who have sex with men in 9 Chinese cities. *J Acquir Immune Defic Syndr* 2013;**64**(1):16–24.

Xi Li<sup>1#</sup>

Department of AIDS Research, State Key Laboratory of Pathogen and Biosecurity, Beijing Institute of Microbiology and Epidemiology, Beijing 100071, China

Jianjun Wu<sup>1#</sup>

Anhui Provincial Center for Disease Control and Prevention, Hefei 230601, China

Yu Zhang

Department of AIDS Research, State Key Laboratory of Pathogen and Biosecurity, Beijing Institute of Microbiology and Epidemiology, Beijing 100071, China

Yuelan Shen

Anhui Provincial Center for Disease Control and Prevention, Hefei 230601, China

Hanping Li

Department of AIDS Research, State Key Laboratory of Pathogen and Biosecurity, Beijing Institute of Microbiology and Epidemiology, Beijing 100071, China

Hui Xing

State Key Laboratory for Infectious Disease Prevention and Control, National Center for AIDS/STD Control and Prevention, Chinese Center for Disease Control and Prevention, Beijing 102206, China

Yongjian Liu

Department of AIDS Research, State Key Laboratory of Pathogen and Biosecurity, Beijing Institute of Microbiology and Epidemiology, Beijing 100071, China

Xiaohui Yang, Xinping Ding, Bing Hu

Fuyang Center for Disease Control and Prevention, Fuyang 236069, China

Jingwan Han, Jingyun Li  
Department of AIDS Research, State Key Laboratory of Pathogen and  
Biosecurity, Beijing Institute of Microbiology and Epidemiology,  
Beijing 100071, China

Bin Su  
Anhui Provincial Center for Disease Control and Prevention, Hefei  
230601, China

Xiaolin Wang\*, Lin Li\*  
Department of AIDS Research, State Key Laboratory of Pathogen and  
Biosecurity, Beijing Institute of Microbiology and Epidemiology,  
Beijing 100071, China

\*Co-Corresponding authors.  
E-mail address: [dearwood@sina.com](mailto:dearwood@sina.com) (L. Li)

<sup>1</sup> #Xi Li and Jianjun Wu contributed equally to this paper.  
Accepted 28 September 2019  
Available online 13 November 2019

<https://doi.org/10.1016/j.jinf.2019.09.022>

© 2019 The Author(s). Published by Elsevier Ltd on behalf of The British Infection Association. This is an open access article under the CC BY-NC-ND license.

## The molecular characteristics of *Neisseria meningitidis* serogroup Y clonal complex 23 first emerge in China



Dear Editor,

Recently, the population structure of invasive *Neisseria meningitidis* (Nm) was assessed after the use of MenACWY among adolescents was recommended since 2005 in the United States.<sup>1</sup> The results show that some CCs such as CC11, CC23 and CC32 clustered more closely to isolates collected from the same continent, exhibiting regional associations. In the United States and Europe,

the *N. meningitidis* serogroup Y clonal complex 23 (CC23) was responsible for the increasing meningococcal disease since the 1990s.<sup>2,3</sup> In China, the meningococcal vaccine A, bivalent vaccine A+C and tetravalent vaccine ACWY had been introduced into the national expanded immunization program in 1980, 2002 and 2008 respectively. While the current incidence of *N. meningitidis* disease in China is mainly caused by serogroups A, B and C, only some sporadic cases caused by the serotypes of X and W135 in recent years.<sup>4,5</sup> In our disease surveillance system, we have never found a case infected with *N. Meningitidis* serogroup Y CC23 before.

Here we report the first case infected with *N. meningitidis* serogroup Y CC23, as well as some characteristics of the strains isolated from the patient and his close contact in China. The patient was a 17-year-old male high school student who was admitted to a local hospital in Guangdong in March 2019. He had been studying and accommodating in the school for a week before the onset of the disease. He had never traveled abroad or contacted with foreigners recently, and his main activities were in classrooms, dormitories and student cafeteria. He had been vaccinated with one dose of A+C bivalent meningococcal vaccine when he was 5 years old. The infection started with sudden high fever (40 °C) on the evening of March 6, 2019. Nausea, vomiting, and limb weakness developed, and the patient lost consciousness on the morning of March 7, 2019. Physical examinations showed Kernig signs, Brudzinski signs. Cerebrospinal fluid (CSF) samples were turbid with increased protein levels (>3000 mg/L) and pressure; leukocyte count also increased ( $7795 \times 10^6/L$ ). After treated with combination of meropenem and vancomycin, the patient was fully recovered in March 8, 2019. In the epidemiological investigation, one of his close contact, also a 17-year-old male high school student, the roommate of the patient, was identified as an asymptomatic carrier.

Two *N. meningitidis* strains were isolated from patient's blood (N19-2-Y) and close contact's throat swab (N19-3-Y) samples respectively. The isolates were identified as serogroup Y by both specific antiserum (Remel, Lenexa, KS, USA) and *SiaD* PCR. The antibiotic susceptibility test was performed following the CLSI guide, and both of the two isolates of *N. meningitidis* serogroup Y were sensitive to all the antibiotics tested excepting nalidixic acid.

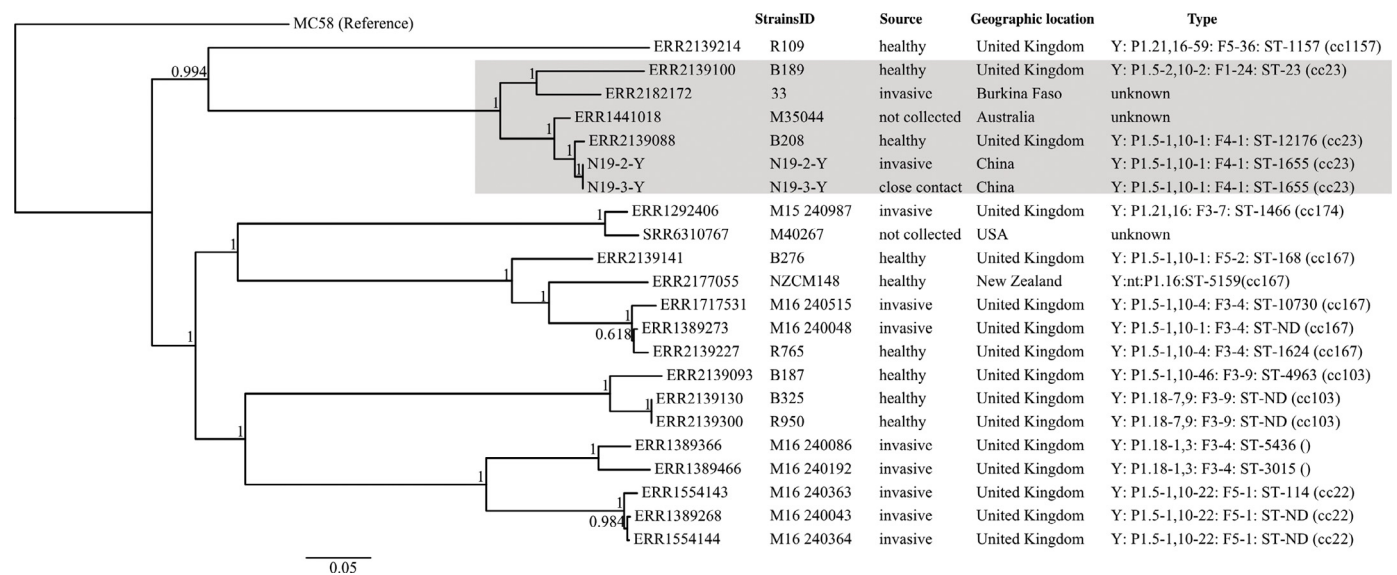


**Fig. 1.** Phylogenies of lineages of *Neisseria meningitidis* Serogroup Y strains by wgSNPs analysis. Phylogenetic analysis revealed that N19-2-Y and N19-3-Y were clustered into CC23 cluster and closest to a United Kingdom strain, which was isolated from healthy people. The *PorA* genotype of the strain was determined to be P1.5-1 and the *porB* and *fetA* alleles of these strains were 10-1 and F4-1, respectively.

**Table 1**  
Summary of snp difference of *Neisseria meningitidis* Y isolates.

| Similarity_matrix | ERR1441018 | ERR2139088 | N19-3-Y | N19-2-Y | NC_003112 | ERR2182172 | ERR2139100 |
|-------------------|------------|------------|---------|---------|-----------|------------|------------|
| ERR1441018        | 100        | 83.85      | 83.38   | 83.38   | 58.15     | 45.65      | 34.2       |
| ERR2139088        | 83.85      | 100        | 93.08   | 93.08   | 57.77     | 42.06      | 29.75      |
| N19-3-Y           | 83.38      | 93.08      | 100     | 99.98   | 58.35     | 41.72      | 29.45      |
| N19-2-Y           | 83.38      | 93.08      | 99.98   | 100     | 58.35     | 41.72      | 29.45      |
| NC_003112         | 58.15      | 57.77      | 58.35   | 58.35   | 100       | 53.27      | 52.58      |
| ERR2182172        | 45.65      | 42.06      | 41.72   | 41.72   | 53.27     | 100        | 44.73      |
| ERR2139100        | 34.2       | 29.75      | 29.45   | 29.45   | 52.58     | 44.73      | 100        |
| difference_matrix | ERR1441018 | ERR2139088 | N19-3-Y | N19-2-Y | NC_003112 | ERR2182172 | ERR2139100 |
| ERR1441018        | 0          | 1548       | 1593    | 1593    | 4012      | 5210       | 6308       |
| ERR2139088        | 1548       | 0          | 663     | 663     | 4048      | 5554       | 6734       |
| N19-3-Y           | 1593       | 663        | 0       | 2       | 3993      | 5587       | 6763       |
| N19-2-Y           | 1593       | 663        | 2       | 0       | 3993      | 5587       | 6763       |
| NC_003112         | 4012       | 4048       | 3993    | 3993    | 0         | 4480       | 4546       |
| ERR2182172        | 5210       | 5554       | 5587    | 5587    | 4480      | 0          | 5298       |
| ERR2139100        | 6308       | 6734       | 6763    | 6763    | 4546      | 5298       | 0          |

We investigated these two *N. meningitidis* strains by whole genome sequencing and submitted the whole genome data to *Neisseria spp.* database on <https://pubmlst.org/>. The fine types were extracted from whole genome data. Both invasive and carried strains were ST-1655, belonging to the ST-23 clonal complex (CC23), which was responsible for an increasing meningococcal disease since the 1990s in the United States and Europe. The *PorA* genotype of the strain was determined to be P1.5-1, which was a genotype specific to the CC23. The *porB* and *fetA* alleles of these strains were 10-1 and F4-1, respectively (Fig. 1). There were only two SNPs between whole genome sequences of N19-2-Y and N19-3-Y (Table 1). Phylogenetic analysis revealed that these two isolates were clustered into CC23 cluster and closest to a United Kingdom strain, which was isolated from healthy people (Fig. 1). There were 663 to 6734 SNPs between our strains and other CC23 strains, suggesting high genetic polymorphisms of CC23 strains (Table 1).

In this study, we report the first case of infection with *Neisseria meningitidis* serogroup Y CC23 in China. This case had never traveled abroad or contacted with suspected cases of meningitis or foreigners before the onset of the disease, so it can be judged as a local infection. By epidemiological case searching and medical examination, we didn't find other similar cases excepted one carrier, suggesting that the ST-23 clonal complex did not spread locally. So far, only one case of *N. meningitidis* serogroup Y ST-175 was reported in China in 2015. However, the *N. meningitidis* serogroup Y CC23 was responsible for an increasing meningococcal disease since the 1990s in the United States and Europe. By 2019, there have been reports of *N. meningitidis* serogroup Y in more than 20 countries, especially in Northern Europe, with the highest proportion up to 55%.<sup>5</sup>

Currently, the *N. meningitidis* strains that caused meningococcal disease mainly belong to serogroups A and C. In China, the meningococcal vaccine A and bivalent vaccine A+C has been introduced into the national expanded immunization program in 1980 and 2002 respectively, which may lead to changes in the prevalence of epidemic serogroups A and C. Survey in Chinese healthy population discovered low positive rate of antibody of *N. meningitidis* serogroups Y, but a high carrier rate of the pathogen.<sup>6–8</sup> Recently, the *N. meningitidis* serogroup Y CC23 was epidemic in the United States and Europe. With the increasing activity of international economic trade and travel, the import risk of *N. meningitidis* serogroup Y CC23 has been accelerated. Thus, our report was useful for improving our understanding of the international spread of

*N. meningitidis* CC23 on a global scale. It also highlights the need for further epidemiologic surveillance to monitor the incidence of meningococcal disease caused by *N. meningitidis* serogroup Y CC23 and improvement of public health disease control strategies in the future.

#### Conflict of interest statement

The authors declare that there are no conflict of interest.

#### Acknowledgment

We thank Zhu BQ for valuable comments and suggestions for preparing the manuscript.

#### Funding source

This work was supported by the Foundation of Medical Science and Technology Research of Guangdong Province, China (No. A2017482).

#### References

- Potts C.C., Joseph S.J., Chang H.Y., Chen A., Vuong J., Hu F., et al. G population structure of invasive *Neisseria meningitidis* in the United States, 2011–15. *J Infect* 2018;**77**(5):427–34. doi:10.1016/j.jinf.2018.06.008.
- Krauland M.G., Hotopp J.C., Riley D.R., Daugherty S.C., Marsh J.W., Messonnier N.E., et al. Whole genome sequencing to investigate the emergence of clonal complex 23 *neisseria meningitidis* serogroup Y disease in the United States. *PLoS ONE* 2012;**7**(4). doi:10.1371/journal.pone.0035699.
- Broker M., Jacobsson S., Kuusi M., Pace D., Simões M.J., Skoczynska A., et al. Meningococcal serogroup Y emergence in Europe: update 2011. *Hum Vaccin Immunother* 2012;**8**(12):1907–11. doi:10.4161/hv.21794.
- Chen C., Zhang T.G., He J.G., Wu J., Chen L.J., Liu J.F., et al. A first meningococcal meningitis case caused by serogroup X *Neisseria meningitidis* strains in China. *Chin Med J (Engl)* 2008;**121**:664–6. doi:10.1097/00029330-200804010-00017.
- Shao Z., Zhou H., Gao Y., Ren H., Xu L., Kan B., et al. *Neisseria meningitidis* serogroup W135, China. *Emerg Infect Dis* 2010;**16**:348–9. doi:10.3201/eid1602.090901.
- Luo X., Zhang W., Chen W., Huang H., Gao Z. Investigation of antibody level against *Neisseria meningitidis* W135 and Y in healthy population in Tianjin, 2016. *Dis Surveill (Chin)* 2018;**33**(07):569–72. doi:10.3784/j.issn.1003-9961.2018.07.009.
- Zhan X., Wang X., Huang H., Jing Y. Antibody level against epidemic cerebrospinal meningitis serogroup Y and serogroup W135 in healthy. *Chine J Public Health (Chin)* 2010;**26**(07):939–40.
- Gong J., Li C., Quan Y., Liao H., Fang J., Huang G., et al. Serogroup Y meningitis carriage and antibody levels among natural population in Guangxi. *J Appl Prev Med (Chin)* 2010;**16**(02):68–70. doi:10.3969/j.issn.1673-758X.2010.02.002.

Baisheng Li<sup>1</sup>

*Center for Disease Control and Prevention of Guangdong Province,  
China*

Liping Zhang<sup>1</sup>

*Center for Disease Control and Prevention of Dongguan, Guangdong,  
China*

Meizhen Liu

*Center for Disease Control and Prevention of Guangdong Province,  
China*

Xueyi Ye

*Center for Disease Control and Prevention of Dongguan, Guangdong,  
China*

Xin Xu, Zhencui Li, Wenjia Liang, Jieli Deng, Limei Sun, Jie Wu

*Center for Disease Control and Prevention of Guangdong Province,  
China*

Qiaoli Zhang\*

*Center for Disease Control and Prevention of Dongguan, Guangdong,  
China*

Tie Song\*

*Center for Disease Control and Prevention of Guangdong Province,  
China*

\*Corresponding authors.

E-mail addresses: [zql@dg.gov.cn](mailto:zql@dg.gov.cn) (Q. Zhang), [tsong@cdcp.org.cn](mailto:tsong@cdcp.org.cn) (T. Song)

<sup>1</sup> Both authors contributed equally to this work.

Accepted 3 July 2019

Available online 13 November 2019

<https://doi.org/10.1016/j.jinf.2019.07.001>

© 2019 The British Infection Association. Published by Elsevier Ltd. All rights reserved.